

Chapter 3 Effect of Geometric Nonlinearities on Cylinder Response

The differences between linear and nonlinear analyses are strictly due to the nonlinear terms in the strain-displacement equations, as given by the underlined terms in eq. 1.7a-c. This chapter examines the differences between linear and nonlinear analyses created by these nonlinear terms. For this comparison a quasi-isotropic laminate is again chosen, and responses are evaluated using both geometrically linear and geometrically nonlinear analyses, but for just an elliptical cylinder. The effects of geometric nonlinearities are shown using three different types of figures. The first type is a three-dimensional format illustrating the response of one-eighth of the cylinder, as in the previous chapter. The coordinate locations range from $0 \leq x/L \leq 0.5$ and $0 \leq s/C \leq 0.25$. The remaining types are two-dimensional in format, with the desired response plotted as a function of x/L or s/C . These two-dimensional format graphs show a comparison of linear and nonlinear analyses along a line at a particular s/C or x/L location for the purpose of a closer examination of an issue that may be difficult to discern from a three-dimensional format. A comparison of linear and nonlinear analyses are shown only for responses that display significant differences, not all responses.

3.1 Displacements

Recall from the boundary conditions of eq. 1.3 that the axial displacement is zero at $x/L = -0.5$, and at $x/L = 0.5$ the axial displacement is determined by eq. 1.4. Recall also that for the linear analysis, and as was discussed earlier in connection with fig. 2-2b, the axial displacement at $x/L=0$

is practically independent of s and it is one-half the value of the axial displacement at $x/L=0.5$. This factor of two also exists for the nonlinear case. However, the magnitude of the axial displacement response differs for the two analyses. As seen in fig. 3-1 and fig. 3-2, the nonlinear analysis requires a slightly smaller axial end displacement, or Δ , to satisfy the axial equilibrium given in eq. 1.4. Figure 3-1 is a three-dimensional format figure and fig. 3-2 is a two-dimensional format figure with the axial displacement given as a function of x/L at two different s/C locations, $s/C = 0.0$ and 0.25 . Though the overall characters of the axial displacement responses are the same for linear and nonlinear analyses, the displacement difference at $x/L = 0.5$ is evident. The existence of negative axial displacements is also clearly seen in this figure.

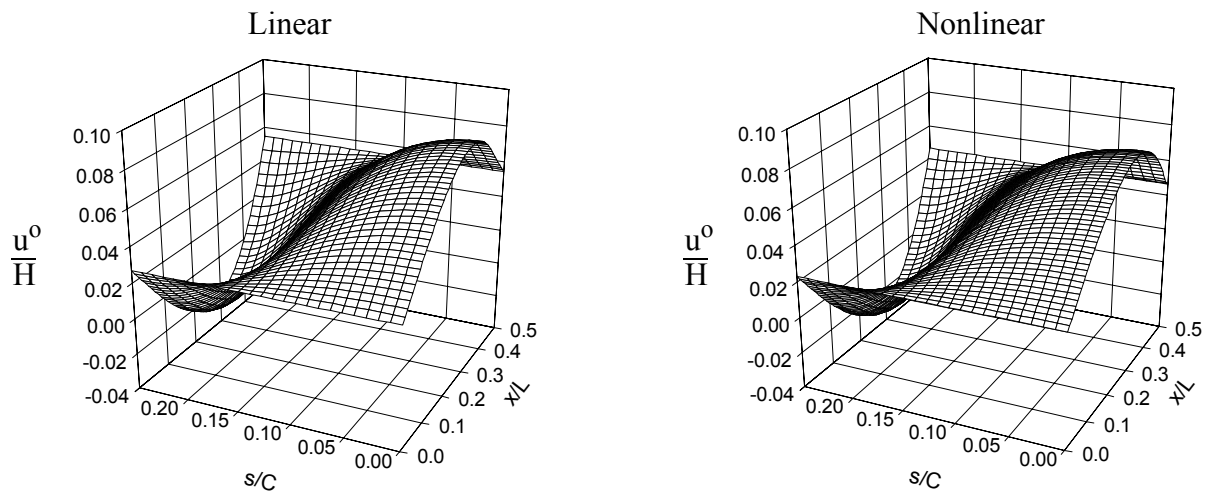


Figure 3-1. Effect of geometric nonlinearities on the axial displacement.

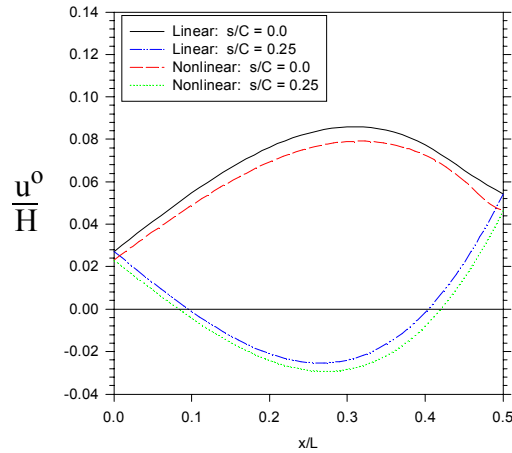


Figure 3-2. Effect of geometric nonlinearities on the axial displacement: linear vs. nonlinear at $x/L = 0$.

Comparing linear and nonlinear analyses, the circumferential displacements appear almost identical as shown in fig. 3-3. However, when circumferential displacements are plotted as a function of s/C along $x/L = 0$ (midspan), as in fig. 3-4, a difference in the displacement magnitudes is detected. For the linear analysis, the extreme value of v^o/H is -0.4918 and it is located at $s/C = 0.1458$. For the nonlinear analysis, the extreme value of v^o/H is -0.4633 and it is located at $s/C = 0.1563$. In short, the extreme circumferential displacement in the nonlinear analysis is smaller in magnitude by approximately 5.8%, and is also shifted approximately 6.7% towards the side of the cylinder.

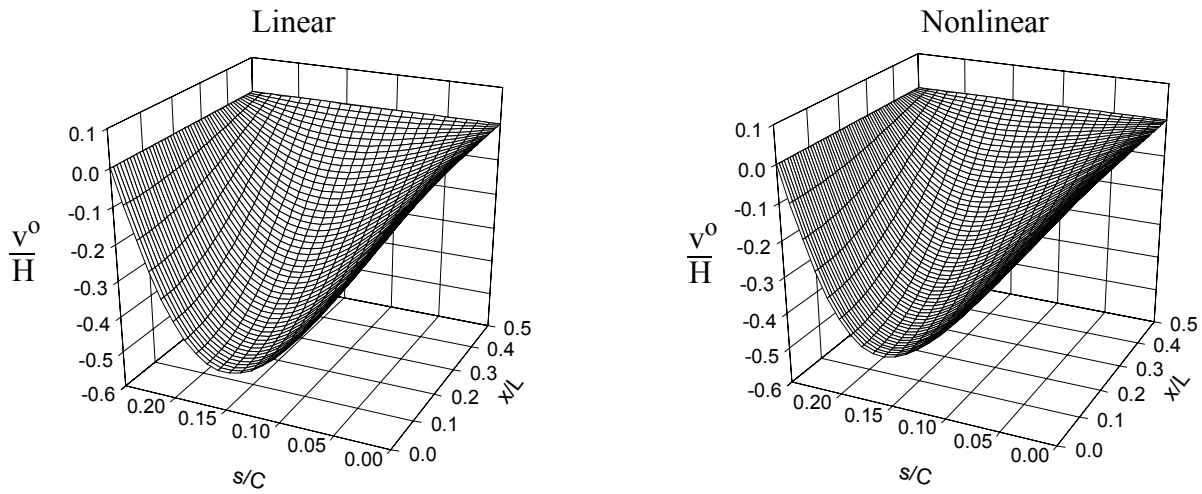


Figure 3-3. Effect of geometric nonlinearities on the circumferential displacement.

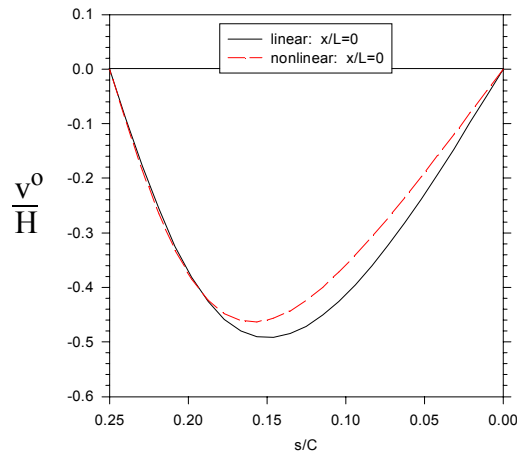


Figure 3-4. Effect of geometric nonlinearities on the circumferential displacement: linear vs. nonlinear at $x/L = 0$.

The normal displacement, shown in fig. 3-5 and fig. 3-6, tends to ‘flatten’ relative to the linear analysis when evaluated using a nonlinear analysis. The normal displacement, as seen in fig. 3-6, evaluated using a nonlinear analysis moves outward less in the crown region, represented by $0 \leq s/C \leq 0.10$, than does the normal displacement evaluated using a linear analysis. This is due to the effect of N_s coupling with w^o through geometrically nonlinear effects.

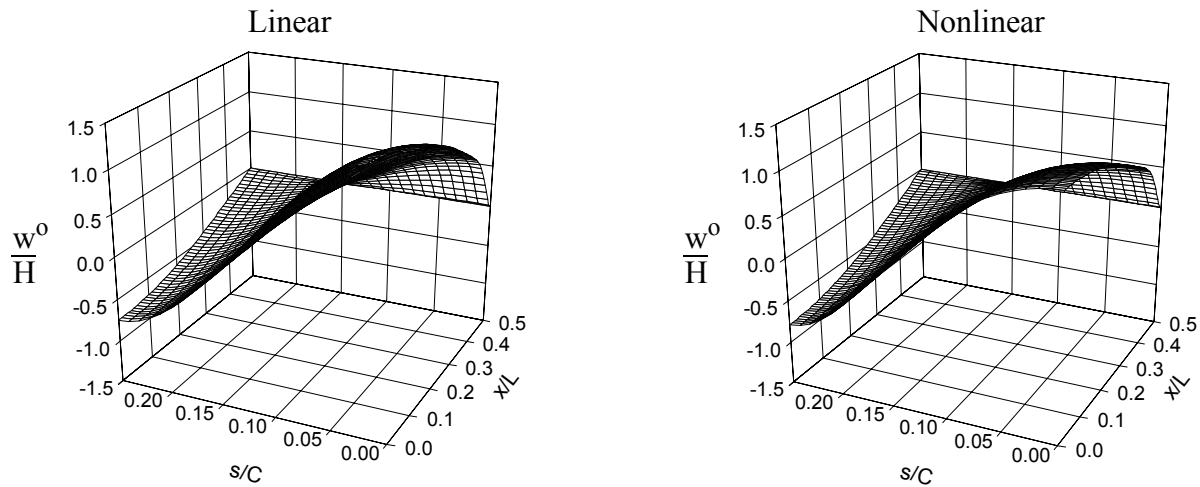


Figure 3-5. Effect of geometric nonlinearities on the normal displacement.

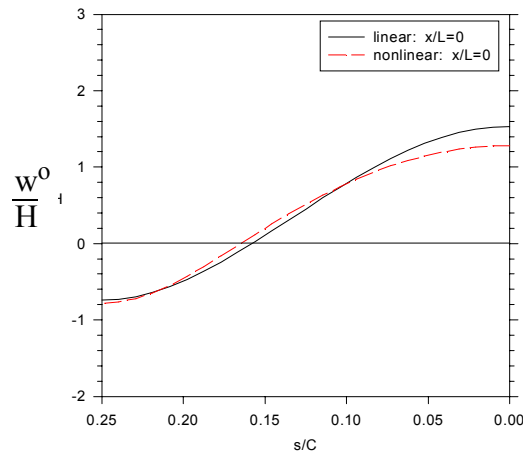


Figure 3-6. Effect of geometric nonlinearities on the normal displacement: linear vs. nonlinear at $x/L = 0$.

All strain, curvature, and force and moment resultant responses can be expressed in terms of the displacements, and as just shown in fig. 3-1 through fig. 3-6, each of the displacements predicted using a nonlinear analysis varies from the displacements predicted using a linear analysis. Therefore, each of these displacement-dependent responses can be expected to also vary using a

nonlinear analyses. However, some responses show little difference between linear and nonlinear analyses. To follow is a discussion of the responses that do show differences.

3.2 Strains and Curvatures

The circumferential strain for the nonlinear analysis follows the same trend as the circumferential strain for the linear analysis, as seen in fig. 3-7 and fig. 3-8. However, the circumferential strain at the crown of the cylinder using the nonlinear analysis does not reach the same magnitude as the circumferential strain at the crown of the cylinder using the linear analysis. The nonlinear circumferential strain from eq. 1.7a depends on the variation of ν^o with s , w^o , the inverse radius of curvature, and an additional nonlinear term which is the square of the variation of w^o with s . As seen earlier, the normal displacement, w^o , experiences a ‘flattening’ effect, which causes w^o and the variation of w^o with s to be smaller in magnitude at the crown of the cylinder. Also, ν^o shows a reduction in magnitude, which lessens the magnitude of the variation of ν^o with s . All of these reactions to a nonlinear analysis combine to result in a lower magnitude for $\bar{\epsilon}_s^o$. The differences between linear and nonlinear analyses for the axial strain and shear strains, from eq. 1.7a and c, appear to be negligible as compared with the difference in the circumferential strains.

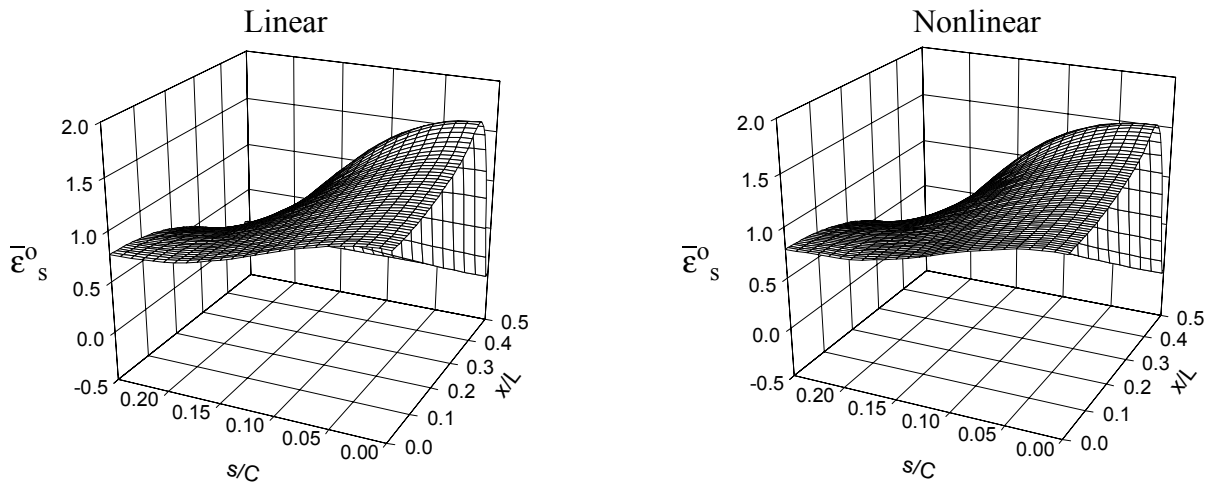


Figure 3-7. Effect of geometric nonlinearities on the circumferential strain.

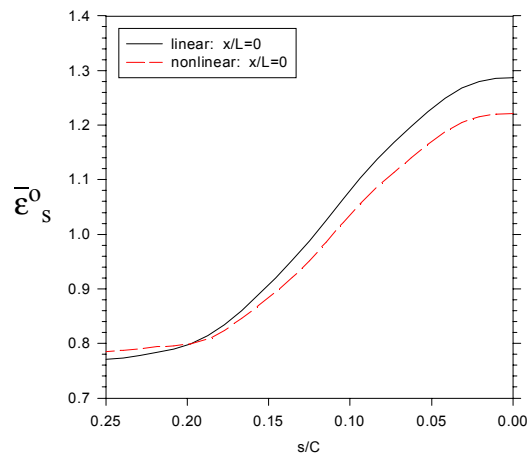


Figure 3-8. Effect of geometric nonlinearities on the circumferential strain: linear vs. nonlinear at $x/L = 0$.

The differences between linear and nonlinear analyses for circumferential curvature are easily visible in fig. 3-9 and fig. 3-10. In the midspan region for the nonlinear analysis case, there is a significant ‘flattening’ along the crown of the cylinder. The definition for circumferential curvature, given in eq. 1.7e as the second derivative of w^o with respect to the s coordinate, is the same for both the linear and nonlinear analyses. As the normal displacement experiences a ‘flat-

tening' effect at the crown, the circumferential curvature also tends to 'flatten' at the crown of the cylinder.

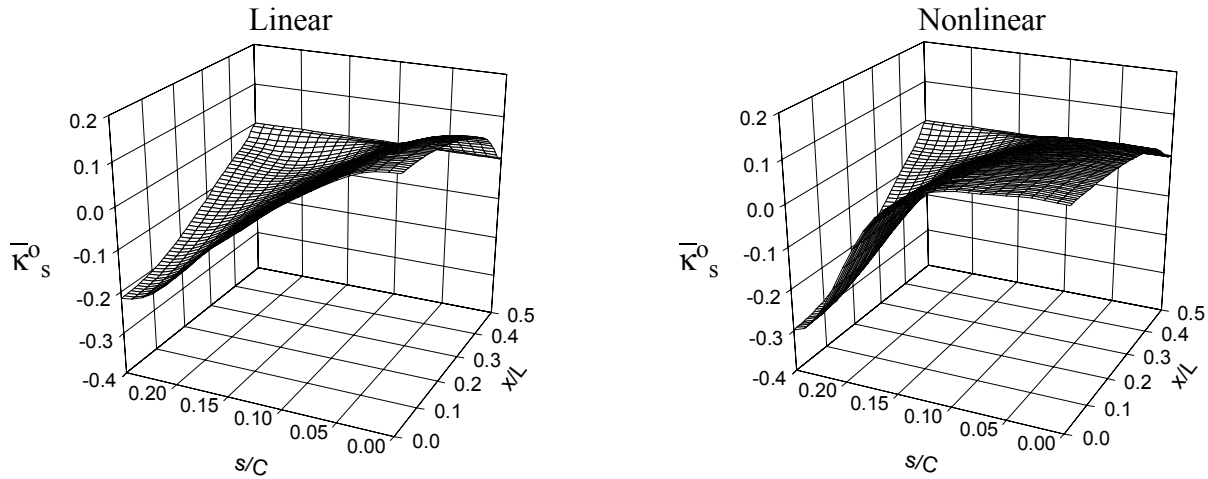


Figure 3-9. Effect of geometric nonlinearities on the circumferential curvature.

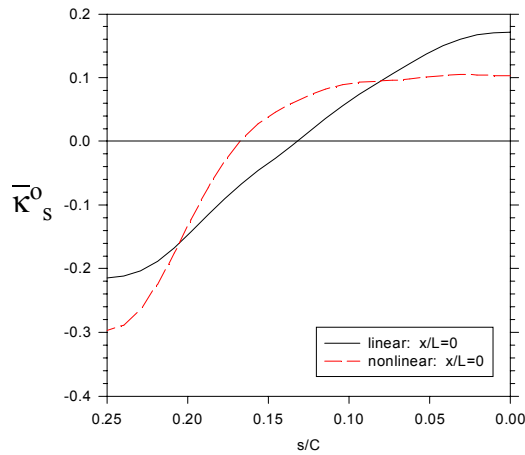


Figure 3-10. Effect of geometric nonlinearities on the circumferential curvature: linear vs. nonlinear at $x/L = 0$.

The differences between linear and nonlinear analyses for axial curvature, as seen in fig. 3-11 and fig. 3-12, are slight in comparison to differences in the circumferential curvature. In the midspan region there is virtually no difference, both analyses predicting zero axial curvature. The

differences between linear and nonlinear analyses for axial curvature exists almost solely in the boundary region, where the axial curvature experiences a change in sign. For the nonlinear case, at the boundary, fig. 3-12, the magnitude of the positive and negative axial curvatures changes slightly, such that the sides have more curvature and the crown and keel have less, and thus the point where axial curvature changes sign moves circumferentially. The influence of the nonlinearities on the axial curvature is explained as follows: The definition for axial curvature, given in eq. 1.7d as the second derivative of w^o with respect to the x coordinate, is the same for linear and nonlinear analysis. The boundary conditions given in eq. 1.3 require that w^o and $\frac{\partial w^o}{\partial x}$ be zero at the end. Since by fig. 3-6 the magnitude of w^o at the crown is less for the nonlinear case, the axial curvature has less to overcome in order to enforce these boundary conditions at the crown of the cylinder. On the other hand, again referring to fig. 3-6, the magnitude of w^o at the sides of the cylinder is slightly greater for the nonlinear analysis as compared to the linear analysis. Therefore, the axial curvature for the sides is slightly greater for nonlinear case.

The differences between linear and nonlinear analyses for twist curvature is not significant compared to the circumferential and axial curvatures.

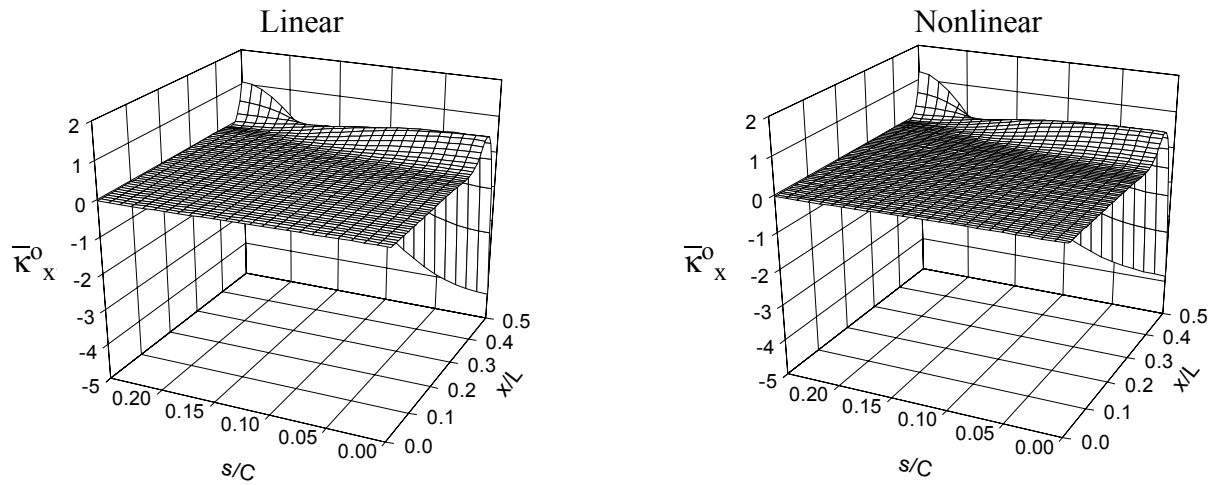


Figure 3-11. Effect of geometric nonlinearities on the axial curvature.

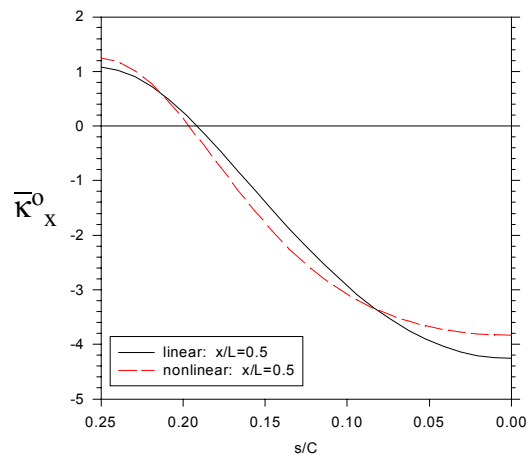


Figure 3-12. Effect of geometric nonlinearities on the axial curvature: linear vs. nonlinear at $x/L = 0.5$.

3.3 Force and Moment Resultants

The nonlinear circumferential force resultant follows the same trend as the linear circumferential force resultant, as seen in fig. 3-13 and fig. 3-14. However, the circumferential force resultant at the crown of the cylinder using nonlinear analysis does not reach the same magnitude as the circumferential force resultant at the crown of the cylinder using linear analysis. This is the

same behavior as seen for circumferential strain, fig. 3-8, which, as seen in eq. 1.9b, is a part of the circumferential force resultant. The axial force resultant shows this same reduction at the crown of the cylinder, although the reduction is less significant, and it is also due to the differences between linear and nonlinear analyses for the circumferential strain. The differences between linear and nonlinear analyses for the shear force resultant are not significant compared to the differences for the circumferential and axial force resultants.

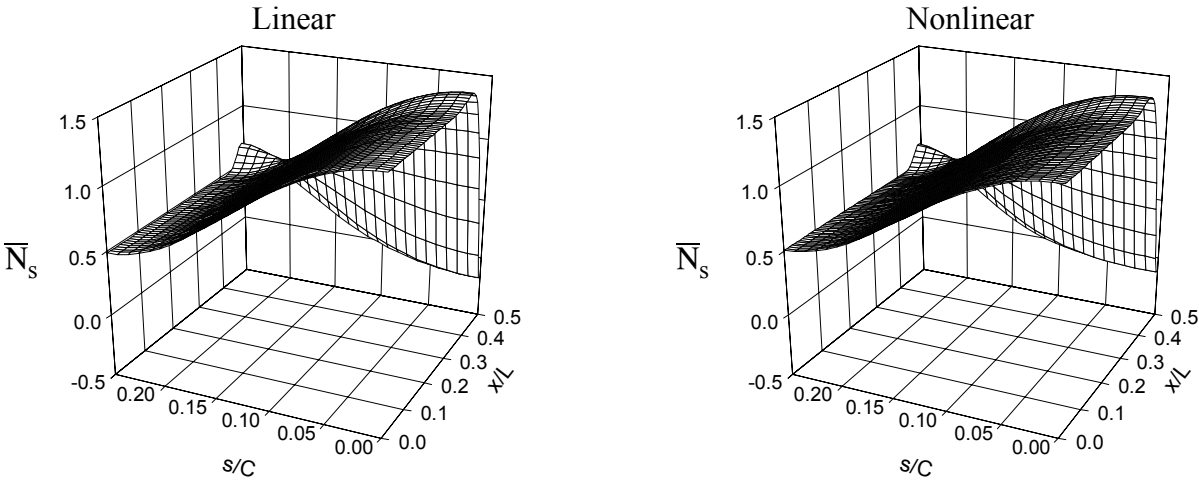


Figure 3-13. Effect of geometric nonlinearities on the circumferential force resultant.

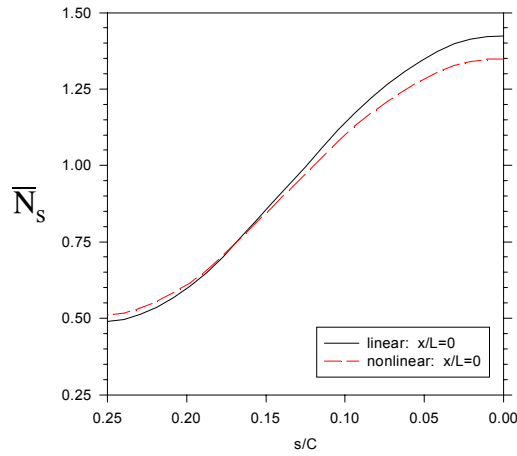


Figure 3-14. Effect of geometric nonlinearities on the circumferential force resultant: linear vs. nonlinear at $x/L = 0$.

The differences between linear and nonlinear analyses for circumferential moment resultant, as seen in fig. 3-15 and fig. 3-16, are found in both the midspan and boundary regions. In the midspan region for the nonlinear case, there is a reduction in the crown region of the cylinder, and an increase in the side region, as was seen with the circumferential curvature of fig. 3-10. Also, there is a change in the response at the ends due to nonlinear analysis, as was seen with axial curvature. However, the difference in response between linear and nonlinear analyses in the boundary region is significantly less than the difference in response in the midspan region. The definition for circumferential moment resultant, given in eq. 1.9e as a linear combination of $\bar{\kappa}_{s,s}^o$, $\bar{\kappa}_{x,x}^o$, and $\bar{\kappa}_{x,s}^o$, is the same for linear and nonlinear analysis. Since $\bar{\kappa}_{s,s}^o$ and $\bar{\kappa}_{x,x}^o$ are both a part of the circumferential moment resultant, the differences between linear and nonlinear analyses from each of these curvatures are reflected in the difference for the circumferential moment resultant. Although not shown here since they are small, the same reasoning applies to differences there are in the axial and twist moment resultants.

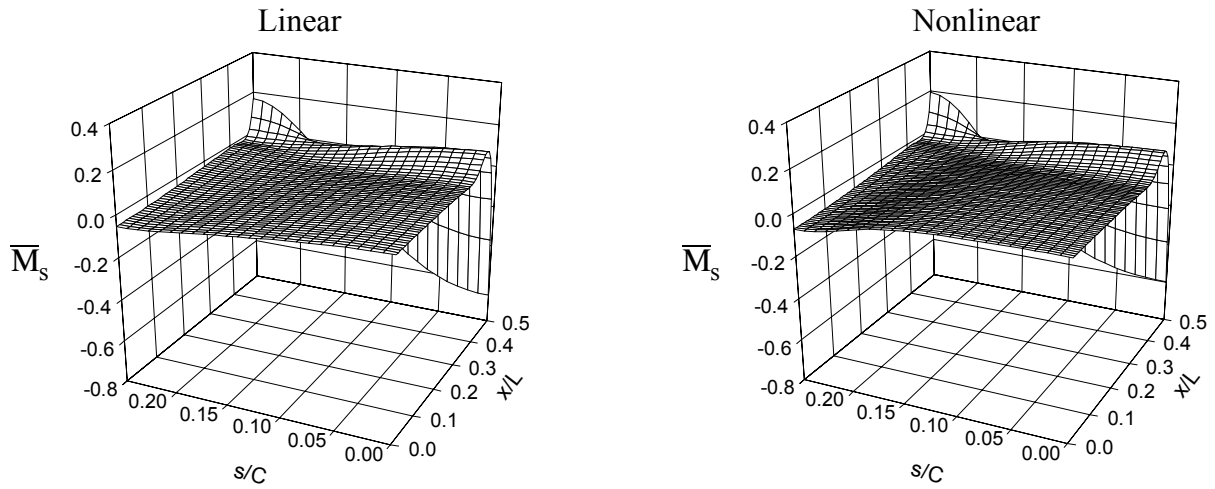


Figure 3-15. Effect of geometric nonlinearities on the circumferential moment resultant.

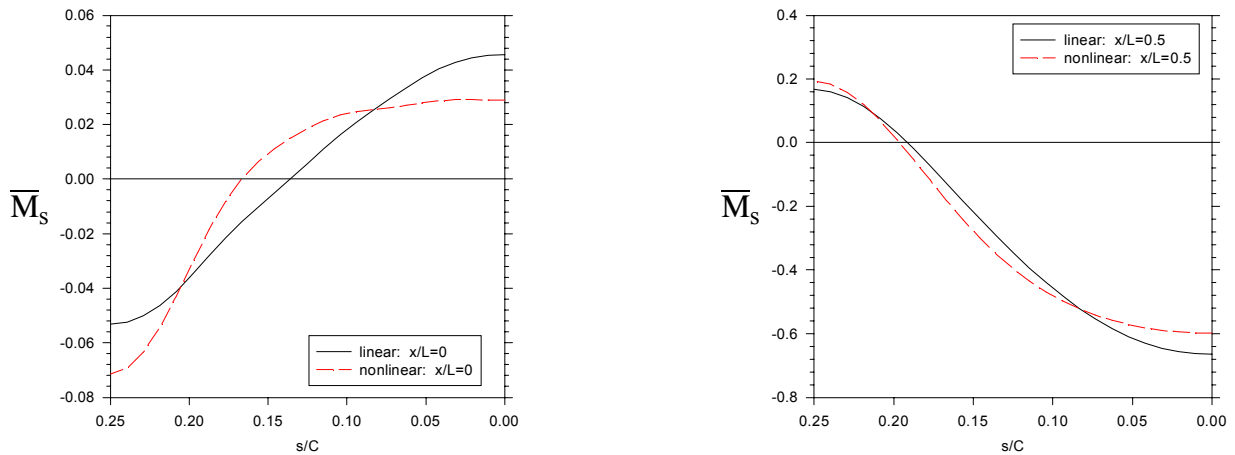


Figure 3-16. Effect of geometric nonlinearities on the circumferential moment resultant: linear vs. nonlinear at $x/L = 0$ and 0.5 .

The transverse shear force resultants, \bar{Q}_s and \bar{Q}_x , seen in figs. 3-17 and 3-18, and figs. 3-19 and 3-20, are defined in eq. 2.6 and depend on the moment resultants. As seen with the moment resultants, the difference between linear and nonlinear analyses occurs mostly in the boundary region. The magnitude of the peaks of the transverse shear force resultants at or near the sides are higher for the nonlinear case, while near the crown they are lower. Most noteworthy for \bar{Q}_s is the

change in sign at the boundary, and the point at which the sign changes. The circumferential transverse shear force resultant changes sign at $s/C = 0.1250$ for the linear analysis and at $s/C = 0.1458$ for the nonlinear analysis. However, for \bar{Q}_x , the change in sign is at approximately the same s/C location for both analyses.

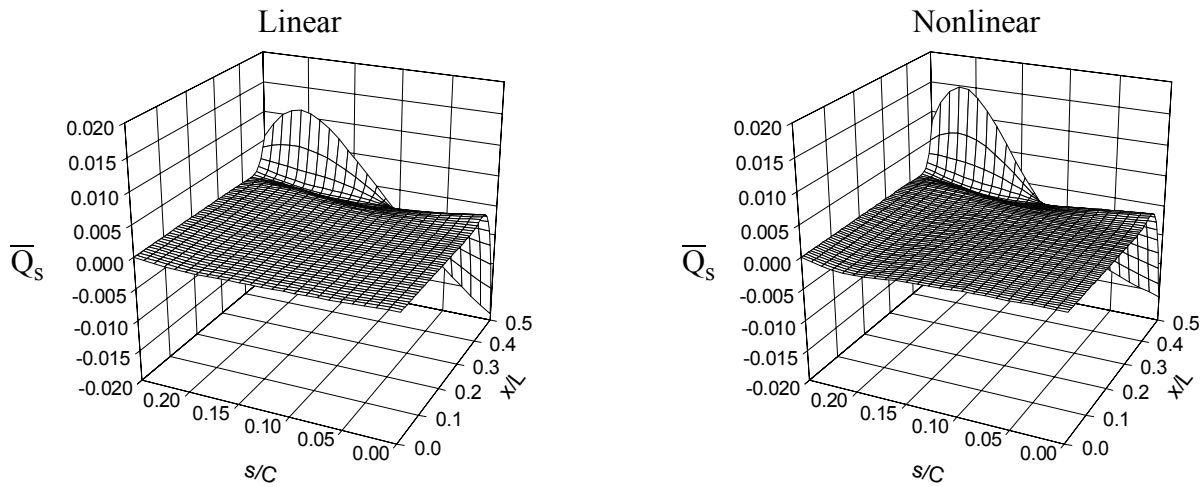


Figure 3-17. Effect of geometric nonlinearities on the circumferential transverse shear force resultant.

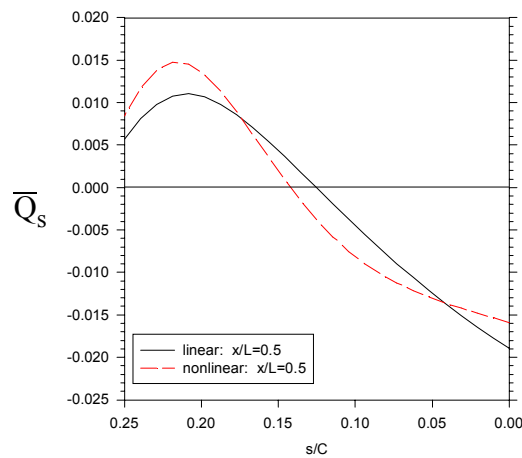


Figure 3-18. Effect of geometric nonlinearities on the circumferential transverse shear force resultant: linear vs. nonlinear at $x/L = 0.5$.

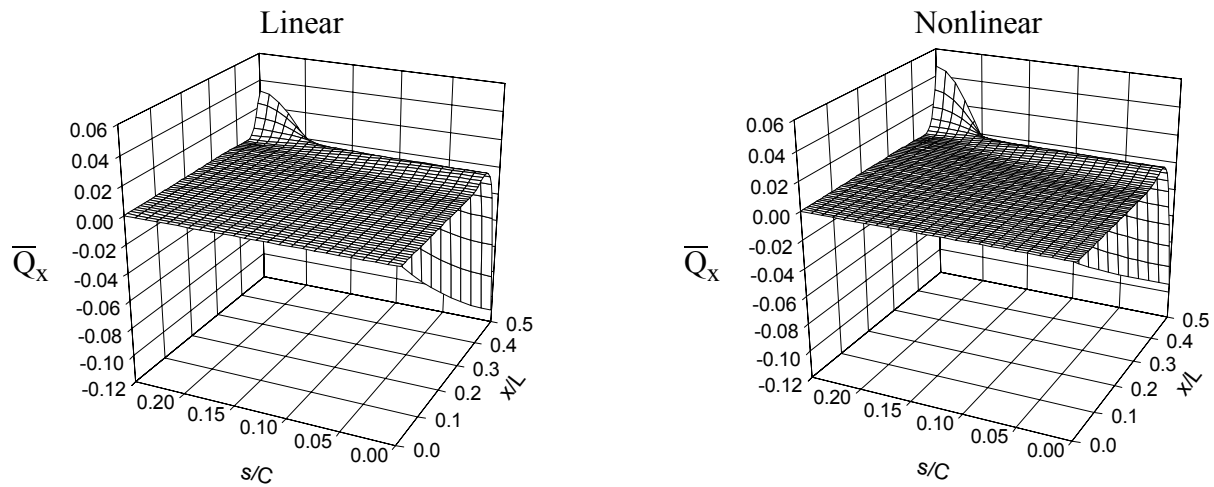


Figure 3-19. Effect of geometric nonlinearities on the axial transverse shear force resultant.

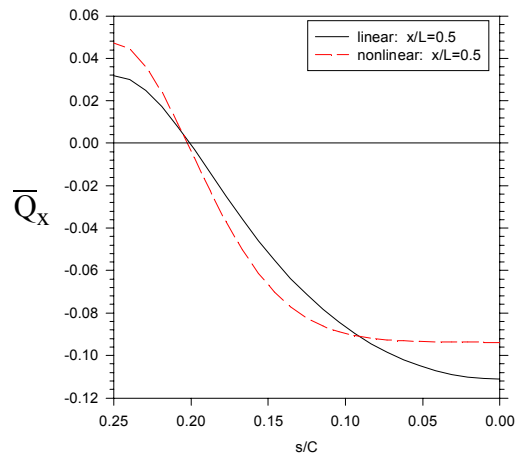


Figure 3-20. Effect of geometric nonlinearities on the axial transverse shear force resultant: linear vs. nonlinear at $x/L = 0.5$.

While \bar{Q}_s and \bar{Q}_x represent the transverse shear force resultant for the linear analysis, there are other transverse force resultants defined for the nonlinear analysis. The \bar{Q}_s and \bar{Q}_x just shown in fig. 3-17 through fig. 3-20 for the nonlinear case have the same definitions as the linear case and they are given in eq. 2.6. These definitions for \bar{Q}_s and \bar{Q}_x for the nonlinear case still represent

transverse shear force resultants. However, they do not act strictly in the outward or inward normal direction, but are rotated away from the normal direction. The transverse force resultants (note the absence of the word ‘shear’) in the normal direction for the nonlinear case are denoted here as V_s and V_x , and are given by,

$$\begin{aligned} V_x &= \frac{\partial M_x}{\partial x} + \frac{\partial M_{xs}}{\partial s} + N_x \frac{\partial w^o}{\partial x} + N_{xs} \frac{\partial w^o}{\partial s} \\ V_s &= \frac{\partial M_{xs}}{\partial x} + \frac{\partial M_s}{\partial s} + N_{xs} \frac{\partial w^o}{\partial x} + N_s \frac{\partial w^o}{\partial s} . \end{aligned} \quad (3.1)$$

These definitions of the transverse force resultants are the consequence of enforcing moment equilibrium for a deformed element of cylinder wall. For the nonlinear analysis V_s and V_x are what is needed to enforce $w^o=0$ at the boundary. As the definition of V_s and V_x include inplane force resultants N_s , N_x , and N_{xs} , and hence σ_s , σ_x , and τ_{xs} , V_s and V_x are not, strictly speaking, shear force resultants in the spirit of eq. 2.7. They are thus referred to as transverse force resultants.

The normalized nonlinear circumferential and axial transverse force resultants, \bar{V}_s and \bar{V}_x respectively, as illustrated in fig. 3-21 and fig. 3-22, are normalized by the same factor used for the force resultants in eq. 2.4. As seen in fig. 3-21, the differences between \bar{Q}_s and \bar{V}_s are significant in all regions. On the other hand, \bar{Q}_x and \bar{V}_x , as in fig. 3-22, have similar behaviors in the midspan and boundary regions. However, the surface of \bar{V}_x near the boundary appears smoother than the surface of \bar{Q}_x .

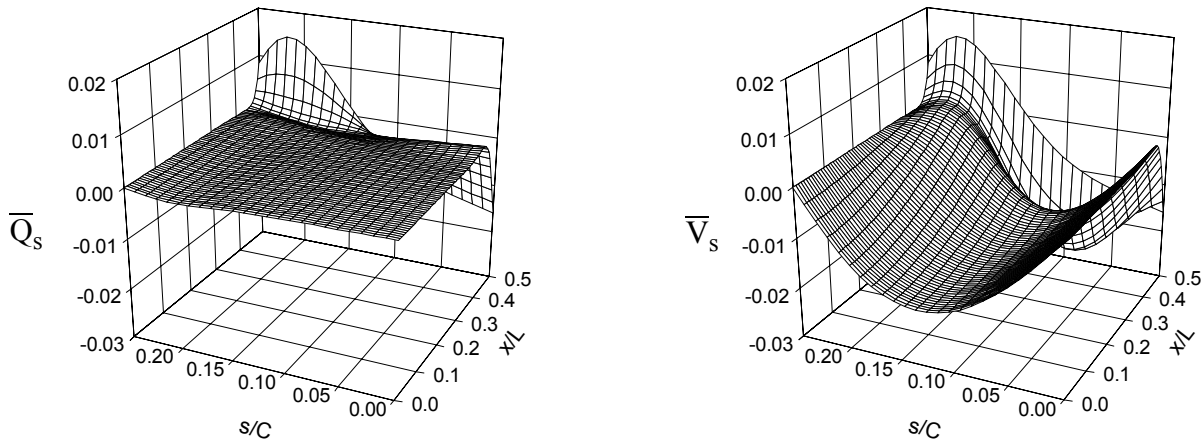


Figure 3-21. Circumferential transverse force resultants.

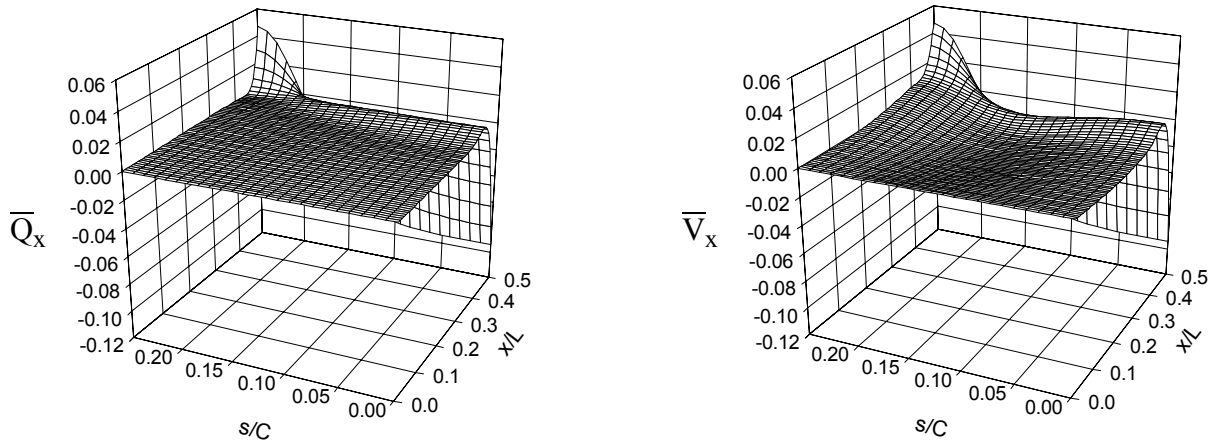


Figure 3-22. Axial transverse force resultants.

3.4 Summary of the Effects of Nonlinearity

The effects of geometric nonlinearities seen in this chapter included several key issues. Between linear and nonlinear analyses, the axial displacement displayed an overall difference in magnitude, the circumferential displacement had a shift in the local minimum, and the normal displacement flattened at the crown of the cylinder. Aside from the displacements, differences between linear and nonlinear analyses, if any exist, seemed to split into two categories, those due

to flattening of the crown of the cylinder, and those involving a change in magnitude of the behavior at the boundary. Flattening of the crown of the cylinder was seen in the circumferential strain, circumferential curvature, and circumferential force resultant. The change of the behavior at the boundary was seen in axial curvature, and axial and circumferential transverse shear force resultants, \bar{Q}_s and \bar{Q}_x . The moment resultants showed both behaviors, a flattening in the crown and a change of magnitude at the boundary. Also, two definitions of the transverse force resultants were introduced. There were significant differences between the circumferential transverse shear force resultant, \bar{Q}_s , and the circumferential transverse force resultant, \bar{V}_s .

The next chapter addresses the consequences of varying the orthotropy of the cylinder. Cylinder responses are compared for axially-stiff, quasi-isotropic, and circumferentially-stiff laminates.